Regular Article

Joint Caching and Hovering Minimized Service Time for Cooperative Video Streaming in UAV-assisted VANETs

Quynh-Anh Nguyen[1], Nguyen-Son Vo[2,4], Van-Ca Phan[3], Dac-Binh Ha[4], Minh-Phung Bui[5], Long D. Nguyen[6]

[1] Vietnam Aviation Academy, Ho Chi Minh City, Vietnam
[2] Institute of Fundamental and Applied Sciences, Duy Tan University, Ho Chi Minh City, Vietnam
[3] Faculty of Electrical and Electronics Engineering, Ho Chi Minh City University of Technology and Engineering, Ho Chi Minh City, Vietnam
[4] Faculty of Electrical-Electronic Engineering, Duy Tan University, Da Nang, Vietnam
[5] Faculty of Information Technology, School of Technology, Van Lang University, Ho Chi Minh City, Vietnam
[6] Dong Nai University, Dong Nai, Vietnam

Correspondence: Nguyen-Son Vo, vonguyenson@duytan.edu.vn
Communication: received 26 December 2025, revised 27 January 2026, accepted 08 February 2026
Online publication: 09 February 2026, Digital Object Identifier: 10.21553/rev-jec.430

Abstract– **The rapid growth of advanced applications and services (A&Ss), particularly video streaming, imposes stringent latency and quality-of-experience requirements on vehicular ad hoc networks (VANETs). Although edge caching at roadside units (RSUs) can reduce service time, its effectiveness is limited in highly dynamic environments characterized by uneven vehicular user (VU) distributions, constrained caching resources, and sparse roadside infrastructure. To address these challenges, this paper proposes a caching and hovering (CAHO) optimization design for cooperative video streaming in VANETs assisted by unmanned aerial vehicles (UAVs). In the proposed CAHO design, VU distributions are modeled as independently thinned one-dimensional homogeneous Poisson point processes, and RSU-to-VU and UAV-to-VU communication models together with video popularity characteristics are incorporated. Based on this modeling, the CAHO problem jointly optimizes video caching at RSUs and UAVs as well as UAV hovering positions to minimize the service time under limited storage resources. The CAHO optimization problem is efficiently solved using genetic algorithms combined with a penalty function and a divide-and-conquer strategy. Simulation results demonstrate that the proposed CAHO scheme outperforms benchmark schemes under various system scenarios in terms of service time and storage resource utilization, highlighting the effectiveness and practical potential for video streaming A&Ss in UAV-assisted VANETs.**

Keywords– **Edge caching, unmanned aerial vehicles, UAV-assisted VANETs, vehicular ad-hoc networks, video streaming applications and services.**

1 Introduction

The proliferation of advanced applications and services (A&Ss) imposes stringent requirements for wireless network infrastructures, posing particular challenges to intelligent transportation systems based on vehicular ad hoc networks (VANETs). The accelerated development of the Internet of Things (IoT), autonomous vehicles, and smart devices, together with multimedia A&Ss, has driven mobile data traffic to exhibit exponential expansion. A statistical report in [1] estimates that approximately 300 million A&Ss will serve 12.3 billion mobile users (MUs), among which video traffic accounts for a dominant share, contributing up to 79% of mobile data traffic [2]. Consequently, the demand for enhanced quality of experience (QoE) from the MUs has grown substantially.

In this context, integrating VANETs with edge techniques emerges as a promising approach to bringing contents and computational resources closer to vehicular users (VUs), thereby mitigating the core network load and reducing the end-to-end latency. Efficient edge caching-enabled techniques play a crucial role in supporting latency-sensitive services, e.g., video streaming A&Ss, by storing popular video contents at the network edge to simultaneously lower service latency and energy consumption [3]. Another study in [4] considers a highly dynamic environment characterized by uneven and dense distribution of VUs, where caching and offloading techniques deployed at roadside units (RSUs) struggle to guarantee quality of service (QoS) under massive and diverse content demands. To address this challenge, the authors designed a joint computation offloading and content caching framework to minimize the overall network delay while satisfying the long-term energy constraints.

For more efficient edge techniques in VANETs, timely studies have proposed cooperative strategies that jointly exploit storage and communication resources at RSUs, macro base station (MBS), and VUs to reduce network congestion and latency [5–7]. Particularly, the authors in [5] proposed a caching scheme

for VANETs that leverages location-based and popular contents, where each content is cached either at both the macro base station (MBS) and RSUs, only at the MBS, or only at RSUs. The objective is to minimize overall transmission delay and service cost. Another work in [6] combines caching at RSUs with broadcast transmission scheduling and transmission rate adaptation to maximize the offloaded traffic. In [7], a joint deterministic and probabilistic caching strategy is proposed for deployment at both RSUs and VUs. Moreover, a cooperative communication framework enabling video delivery from RSUs and VUs to VUs is developed to achieve minimal service time while efficiently utilizing the storage resources of both RSUs and VUs.

Recently, unmanned aerial vehicles (UAVs) have been utilized as an effective augmenting component for VANETs due to their flexibility in selecting hovering positions with a high line-of-sight (LoS) probability, extended communication coverage, and rapid deployment. UAVs can act as aerial base stations to assist VANETs in delivering contents over areas where RSUs are overloaded or terrestrial infrastructure is insufficient [8, 9], [10–12]. In line with this approach, several studies [13–15] have exploited UAVs to design routing protocols and temporal data dissemination algorithms for mitigating post-disaster communication disruptions and delay-sensitive constraints in VANETs. When caching considered, the work [16] deploys UAVs with limited bandwidth resources to assist VANETs. The proposed scheme facilitates content dissemination among VUs through network coding–based cooperative caching to improve bandwidth efficiency. In [17], a UAV is employed to cache content and serve dynamic VUs, with joint trajectory planning and cache management considered to improve the data download amount and energy efficiency. Furthermore, caching can be performed at both UAVs and VUs by jointly utilizing user preferences together with incentive-driven caching and replacement schemes [18]. This solution effectively reduces the request latency and energy consumption.

Other UAV-assisted VANETs with caching have been investigated in the context of human-centric consumer applications, computation offloading, and task offloading [19–21]. However, existing studies in [19, 20] have not fully addressed the joint caching of contents at both RSUs and UAVs for cooperative video streaming A&Ss. Moreover, the determination of UAV hovering positions across diverse wireless propagation environments remains insufficiently investigated, particularly when minimizing service time under constrained caching storage resources. Although caching and replacement schemes at RSUs and UAVs are considered in [21], the hovering positions of UAVs are not taken into account, which limits the achievable delivery efficiency.

In this paper, by modeling the VUs using independently thinned one-dimensional homogeneous Poisson point process (T1D-PPP), incorporating RSU-to-VU (R2V) and UAV-to-VU (U2V) communication models, and capturing video popularity patterns, we propose a caching and hovering optimization (CAHO) design for cooperative video streaming A&Ss. In particular, a CAHO optimization problem is formulated and solved to determine which videos are cached at RSUs and which videos are cached at UAVs associated with their hovering positions to compensate for the caching gaps among RSUs. The objective is to minimize the service time and guarantee continuous video streaming sessions under limited caching storage resources at both RSUs and UAVs. The CAHO optimization problem is solved by using genetic algorithms (GA), combined with a penalty function method and a divide-and-conquer strategy applied to each chromosome-encoded individual. Simulation results show that the CAHO outperforms the other schemes across various system scenarios, thereby demonstrating the effectiveness and practical potential of the proposed solution for video streaming A&Ss in UAV-assisted VANETs.

Table I
Notations

Notations	Specifications
M	Number of UAVs
N	Number of RSUs
K	Number of zones covered by each RSU
I	Number of videos
S_i	Size of video i, $i = 1, 2, ..., I$
p_i	Popularity of video i
h_i	Caching radius of video i in RSUs
s_n	Average speed of VUs in road segment n covered by RU n, $n = 1, 2, ..., N$
b_n	Hovering index, $b_n = 1$ if a UAV hovers at RSU n, otherwise $b_n = 0$
$c_{n,i}$	Caching index of video i in a UAV hovering at RSU n, $c_{n,i} = 1$ if a UAV caches video i and hovers at RSU n, otherwise $c_{n,i} = 0$
d	Distance of a road segment
d_k	Distance of zone k in a road segment
R_k	Transmission rate in zone k in a road segment
λ	Density of VUs
α	Skewed access rate (popularity) exponent among videos
W	System bandwidth
P	Transmission power of UAVs
σ^2	Additive white Gaussian noise power

The rest of this paper is organized as follows. We introduce the system model and describe how it works in Section II. Section III formulates the system model to derive the objective function of the CAHO optimization problem. The CAHO optimization design, i.e., CAHO optimization problem and its solution with GA, is presented in Section IV. In Section V, we evaluate the proposed CAHO method in comparison with other schemes. Finally, Section VI concludes the paper.

2 System Model

In this paper, we deploy a CAHO model for cooperative video streaming in UAV-assisted VANETs as illustrated in Figure 1. The main notations used throughout the paper are summarized in Table I. Along the road, VUs

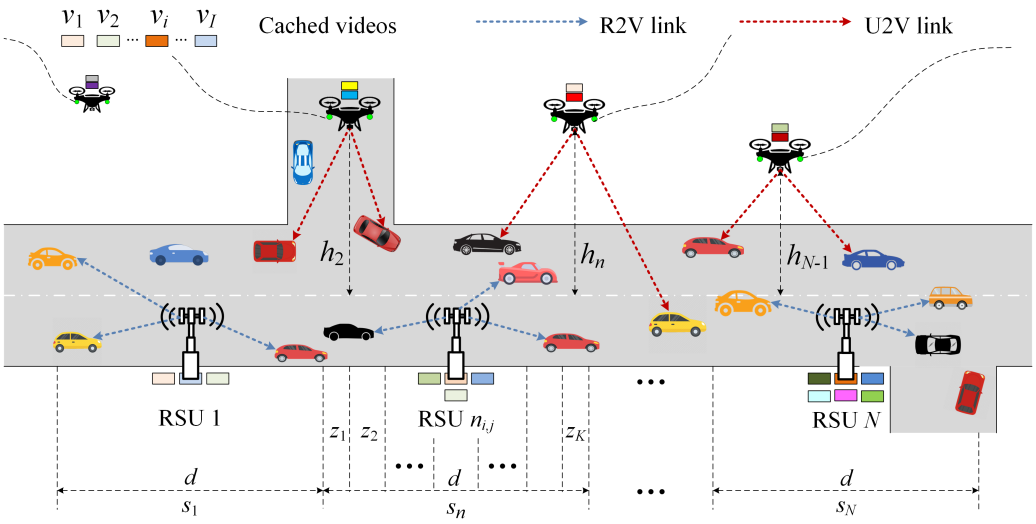

Figure 1. CAHO model for cooperative video streaming in UAV-assisted VANETs.

are spatially distributed according to T1D-PPP Φ with density λ [22, 23]. The road is divided into N segments, and the vehicle speed is assumed to be constant within each segment while varying across different segments, thereby capturing the realistic speed variations caused by traffic conditions, intersections, and driving behaviors. The model consists of N RSUs assisted by M UAVs for video streaming applications and services. There are I videos in the content library, where each video i is characterized by its popularity p_i and size S_i. Each RSU covers a segment of length d meters, which is further divided into K zones. The videos can be cached in both the RSUs and the UAVs. The VUs entering segment n, $n = 1, 2, ..., N$, travel with an average speed of s_n kilometers per hour (km/h). Among the VUs, a subset is defined as requesting vehicular users (RVs) that request the videos.

In this context, to improve the QoS of video streaming A&Ss in VANETs, a CAHO optimization problem is formulated and solved for the optimal results of (i) caching placement (h_i) of video i in the RSUs, (ii) caching placement ($c_{n,i}$) of video i in a UAV hovering over segment n, and (iii) hovering index (b_n) over segment n at altitude h_n. The objective is to minimize the service time while efficiently utilizing the caching storage resources of RSUs and UAVs. The service time is defined as the average duration for the RVs to receive the requested videos from the RSUs and the UAVs while on the move. After deploying the CAHO method, when an RV requests video i, $i = 1, 2, ..., I$, and enters a road segment, it is served by an RSU or a UAV that has cached video i to ensure a more continuous streaming session.

It is noted that if video i (i.e., of large size) cannot be completely transmitted after the RV traverses all N RSUs, the transmission will be continued by a subsequent set of RSUs associated with another MBS. In this work, under moderate network scales, a single MBS can reasonably act as a centralized controller that aggregates network information and disseminates the optimization decisions to associated RSUs and UAVs. For large-scale systems with a high number of RSUs, UAVs, and videos, practical implementation indeed faces two main challenges: (i) the difficulty of collecting timely and accurate system information (e.g., channel state information), and (ii) the increased computational complexity of the optimization algorithms. In such scenarios, the number of RSUs, UAVs, and videos managed by each MBS should be appropriately constrained in accordance with the processing capability of the MBS. Moreover, for larger-scale and highly dynamic VANETs, the proposed CAHO model can be extended to a distributed or cooperative multi-MBS architecture, where multiple MBSs coordinate to serve vehicular users in a scalable manner, similar to the multi-MBS settings considered in prior studies such as [24]. This scenario is beyond the scope of this paper and is left for future investigation. The detailed system formulations for CAHO design and optimization are presented in the sequel.

3 System Formulations

3.1 T1D-PPP Model for RVs

The use of the T1D-PPP model is primarily motivated by its analytical tractability and its ability to provide fundamental insights into the performance trends of large-scale vehicular networks [25, 26]. Several prior works have demonstrated that more complex vehicular models, such as Cox-based models with random road geometries, are equivalent to one-dimensional or two-dimensional PPP models under certain regimes of line density, vehicle density, or signal-to-interference ratio (SIR), particularly in the low-SIR region [27, 28]. In the considered UAV-assisted VANET with caching and video streaming, LoS–dominated links and relatively dense vehicular deployments lead to an interference-limited regime where the SIR thresholds of interest are moderate to low. Furthermore, VUs are associated with nearby caching entities, including road-side units

and UAVs, following proximity-based association rules. As a result, both the desired signal and the dominant interference originate from nearby transmitters along the same road, which aligns well with the assumptions underlying the T1D-PPP model. Given the T1D-PPP model for the spatial distribution of VUs on the one-way roads [22, 23], let p_i be the probability of video i, the distributions of RVs also follow the T1D-PPPs Φ_i^{RV} of density λ_i^{RV}, expressed as

$$\lambda_i^{\mathrm{RV}} = p_i \lambda, \tag{1}$$

where the popularity video i modelled by a Zipf-like distribution [29] is given by

$$p_i = \frac{i^{-\alpha}}{\sum_{l=1}^{I} l^{-\alpha}}, \tag{2}$$

where $\alpha \geq 0$ denotes the coefficient characterizing the skewness of the video popularity distribution; for example, $\alpha = 0$ indicates that all videos have identical popularity.

3.2 Caching at RSUs and UAVs

3.2.1 Caching at RSUs: For caching in RSUs, we define h_i as the caching radius of video i to identify that video i is cached after every h_i hops in RSU $n_{i,j}$, which is computed as

$$n_{i,j} = h_i(j-1) + 1, j = 1, 2, ..., J_i, \tag{3}$$

where J_i is the number of RSUs caching video i, given by

$$J_i = \left\lfloor \frac{N-1}{h_i} \right\rfloor + 1, \tag{4}$$

where the operator $\lfloor . \rfloor$ is used to return the greatest integer less than or equal to a given real number. An example of caching radius $h_i = 5$ is illustrated in Figure 2.

3.2.2 Caching at UAVs: We can see that for particular video i, the number of RSUs that do not cache it is $(N - J_i)$, namely, caching gaps. It is challenging to deploy a large number of UAVs just for caching video i to fulfil the caching gaps. So, given M UAVs, each UAV has to selectively cache a number of videos and hovers above a proper RSU which does not cache them to ensure continuous video streaming sessions (Figure 2). For caching in UAVs, a UAV hovers above RSU $n \neq n_{i,j}$ to transmit video i to the associated RVs if $c_{n,i} = 1$, otherwise $c_{n,i} = 0$.

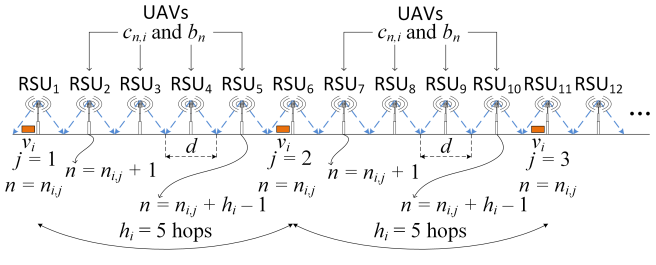

Figure 2. An example of caching placement and hovering with $h_i = 5$.

Table II
Zones Covered by an RU

Zones	1	2	3	4	5	6	7
d_k(m)	25	30	40	60	40	30	25
r_k(m)	125	100	70	30	70	100	125
R_k(Mbps)	1	2	5.5	11	5.5	2	1

3.3 R2V Transmission Capacity

To derive the R2V transmission capacity, we apply the R2V channel model with WiFi access technology given in [5, 30]. In this model, the range d of a road segment covered by an RSU is divided into K zones. The parameters of zone k, $k = 1, 2, ..., K$, $K = 7$, are listed in Table II. The capacity per RV requesting video i in zone k served by RSU n is given by

$$C_{n,k,i}^{\mathrm{R2V}} = \begin{cases} \frac{p_{k,i}^{\mathrm{RV}} R_k}{V_{k,i}}, & \text{if } n = n_{i,j}, \\ 0, & \text{if } n \neq n_{i,j}, \end{cases} \tag{5}$$

where $p_{k,i}^{\mathrm{RV}}$ and $V_{k,i}$ denote, respectively, the probability that at least one RV in zone k requests video i from RSU n and the number of RVs requesting video i within zone k, expressed as

$$p_{k,i}^{\mathrm{RV}} = 1 - e^{-d_k \lambda_i^{\mathrm{RV}}}, \tag{6}$$

and

$$V_{k,i} = d_k \lambda_i^{\mathrm{RV}}. \tag{7}$$

3.4 U2V Transmission Capacity

At RSU $n \neq n_{i,j}$, a UAV hovers above the centerline of the road at altitude h_n and transmits video i to the RVs by following the air-to-ground probabilistic path loss channel [12, 31–33]. We assume that each UAV, which is treated as a common cellular user, is allocated an orthogonal downlink spectrum resource for transmission. Moreover, due to the favorable LoS propagation of U2V links, the impact of interference can be neglected. Under this assumption, mutual interference among U2V links is further mitigated, and thus is not considered in this work. This channel, which is shown in Figure 3, consists of LoS and non-LoS (NLoS) links. The path loss of LoS and NLoS links between a UAV and a typical RV in zone k belonging to RSU n is given by

$$\psi_{n,k}^{\mathcal{A}} = \left(\frac{4\pi f_c d_{n,k}}{c} \right)^2 \eta_n^{\mathcal{A}}, \mathcal{A} \in \{\mathrm{LoS}, \mathrm{NLoS}\}, \tag{8}$$

where f_c is the carrier frequency, c is the speed of light, $\eta_n^{\mathcal{A}}$ is the attenuation factor of LoS link or NLoS link, and similar to the R2V channel model, the worst channel with the longest distance $d_{n,k}$ from the UAV to the RVs remains unchanged when moving in zone k of segment n as shown in Figure 3.

By further considering the occurrence probabilities of the LoS link ($P_{n,k}^{\mathrm{LoS}}$) and of the NLoS link ($P_{n,k}^{\mathrm{NLoS}} = 1 - P_{n,k}^{\mathrm{LoS}}$), we can derive the following average

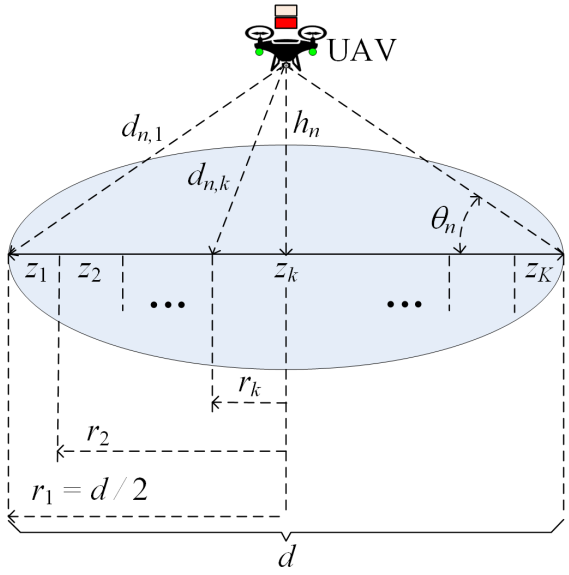

Figure 3. Communication coverage model of a UAV in segment n.

path loss

$$\begin{aligned}\overline{\psi}_{n,k} &= \psi_{n,k}^{\mathrm{LoS}} P_{n,k}^{\mathrm{LoS}} + \psi_{n,k}^{\mathrm{NLoS}} P_{n,k}^{\mathrm{NLoS}} \\ &= \left(\frac{4\pi f_c d_{n,k}}{c}\right)^2 \left(\eta_n^{\mathrm{LoS}} P_{n,k}^{\mathrm{LoS}} + \eta_n^{\mathrm{NLoS}} P_{n,k}^{\mathrm{NLoS}}\right),\end{aligned} \tag{9}$$

where the occurrence probability of the LoS link is given by

$$P_{n,k}^{\mathrm{LoS}} = \frac{1}{1 + \kappa_n \exp\left[-\nu_n\left(\xi_{n,k} - \kappa_n\right)\right]}, \tag{10}$$

where κ_n and ν_n are the constants related to the environment of segment n, $\xi_{n,k} = \frac{180}{\pi} \arctan(\frac{h_n}{r_k})$ [11, 34].

We assume that the UAV, considered as a conventional cellular user, is allocated a downlink spectrum resource for transmission. In the absence of interference, the signal-to-noise ratio of the channel for transmitting video i from the UAV to the RVs in zone k of segment n is given by [31]

$$\gamma_{n,k,i} = \frac{b_n c_{n,i} (\overline{\psi}_{n,k})^{-1} P}{\sigma^2}, \tag{11}$$

where b_n is the hovering index used to decide that a UAV hovers at RSU $n \neq n_{i,j}$ ($b_n = 1$) or does not ($b_n = 0$), $\sum_{n=1, n\neq n_{i,j}}^{N} b_n = M, 1 \leq M \leq N$, and P is the transmission power of the UAV. From (11), we obtain the corresponding capacity expressed as

$$C_{n,k,i}^{\mathrm{U2V}} = \begin{cases} p_{k,i}^{\mathrm{RV}} W \log_2(1 + \gamma_{n,k,i}), & \text{if } n \neq n_{i,j}, \\ 0, & \text{if } n = n_{i,j}, \end{cases} \tag{12}$$

where W is the system bandwidth.

3.5 Average Service Time

In addition, the transmission time to serve the RVs in zone k, i.e., the so-called average time to drive throughout zone k covered by RSU n or a UAV, is simply computed as

$$t_{n,k} = \frac{d_k}{s_n}. \tag{13}$$

By using (13), the average service time for I videos, which is the objective function to be minimized by finding h_i, $c_{n,i}$, and b_n is given by

$$\overline{T} = \sum_{i=1}^{I} p_i t_i, \tag{14}$$

where t_i is the time to cooperatively transmit video i by the RSUs and UAVs presented in Algorithm 1.

Algorithm 1 Computing t_i.

Require: S_i
  $t_i = 0$
Ensure: t_i
1: **for** $j = 1 : J_i$ **do**
2: $n_{i,j} = h_i(j-1) + 1$
3: **for** $k = 1 : K$ **do**
4: **if** $S_i > 0$ **then**
5: $S_i = S_i - C_{n_{i,j},k,i}^{\mathrm{R2V}} t_{n_{i,j},k}$
6: $t_i = t_i + t_{n_{i,j},k}$
7: **else**
8: **break**
9: **end if**
10: **end for**
11: **for** $n = n_{i,j} + 1 : n_{i,j} + h_i - 1$ **do**
12: **if** $n \leq N$ **then**
13: **for** $k = 1 : K$ **do**
14: **if** $S_i > 0$ **then**
15: $S_i = S_i - C_{n,k,i}^{\mathrm{U2V}} t_{n,k}$
16: $t_i = t_i + t_{n,k}$
17: **else**
18: **break**
19: **end if**
20: **end for**
21: **end if**
22: **end for**
23: **end for**

In Algorithm 1, lines 2–10 describe the transmission of video i by RSU $n_{i,j}$. For each zone k, the remaining size S_i is reduced by $C_{n_{i,j},k,i}^{\mathrm{R2V}} t_{n_{i,j},k}$ based on the achievable R2V capacity, and the transmission time t_i is updated (lines 5–6), using (5) and (13). Subsequently, lines 11–22 extend the same procedure to hovering UAVs, where S_i is reduced following the achievable U2V capacity $C_{n,k,i}^{\mathrm{U2V}}$ as defined in (12), and t_i is updated accordingly (lines 15–16). If $S_i > 0$, the transmission time t_i is cumulatively updated in lines 6 and 16, otherwise, Algorithm 1 terminates.

4 CAHO Optimization Design

4.1 CAHO Optimization Problem

Based on the objective function (14) and by further taking the constraint on the caching storage resources of RSUs and UAVs into account, the CAHO optimization

problem is formulated as

$$\min_{h_i, c_{n,i}, b_n} \overline{T}, \tag{15a}$$

$$\text{s.t. } 1 \le h_i \le N-1, \forall i, \tag{15b}$$

$$S^{\text{RSU}} + S^{\text{UAV}} \le \delta N \sum_{i=1}^{I} S_i, \tag{15c}$$

$$\sum_{n=1}^{N} b_n \le M, \tag{15d}$$

where (15c) is used to limit the total storage consumption for caching in RSUs and UAVs, and S^{RSU} and S^{UAV} are the caching storage resources consumed by RSUs and UAVs, respectively computed as

$$S^{\text{RSU}} = \sum_{i=1}^{I} J_i S_i, \tag{16}$$

and

$$S^{\text{UAV}} = \sum_{n=1}^{N} \sum_{i=1}^{I} c_{n,i} b_n S_i. \tag{17}$$

4.2 GA Solution

GA has been widely applied as an effective solution for complicated optimization problems in a broad range of real-world domains [35], spanning from communication systems [36–38] to video streaming A&Ss [39–42]. The effectiveness of GA derives from the evolutionary principles inspired by natural selection and genetic variation. Leveraging these principles, GA can flexibly search for exact or near-global optimal solutions in both unimodal and multimodal search spaces. By exploring multiple peaks of the search space in parallel, GA can avoid local convergence and thus enhance the likelihood of reaching globally optimal solutions [39, 40]. Owing to its robustness, adaptability, and strong global search capability, GA has been extensively used to overcome the challenges of practical optimization problems.

In this paper, we apply GA [43] to solve (15). However, the problem is that GA supports only simple constraints in the form of lower and upper bounds, such as (15b), but not more complex ones like (15c) and (15d). This problem is addressed by using the penalty method [39]. To this end, we convert (15) into an unconstrained optimization problem by reformulating (15c) and (15d) as

$$\begin{cases} \Delta S = \delta N \sum_{i=1}^{I} S_i - S^{\text{RSU}} - S^{\text{UAV}} \ge 0, \\ \Delta M = M - \sum_{n=1}^{N} b_n \ge 0. \end{cases} \tag{18}$$

Then, we derive the penalty function as

$$F = \rho_1 \big(\min\{0, \Delta S\} \big)^2 + \rho_2 \big(\min\{0, \Delta M\} \big)^2, \tag{19}$$

where ρ_1 and ρ_2 are the constraint violation degrees used to adjust the degree of punishment if the individuals in GA violate the constraints.

Finally, GA is capable of solving the following unconstrained CAHO optimization problem

$$\min_{h_i, c_{n,i}, b_n} T_F = \overline{T} + F. \tag{20}$$

The detailed GA used to solve (20) is presented in Algorithm 2. In Algorithm 2, the two integer and binary optimization variables (OVs) cannot be represented by the same chromosome (string) within an individual, nor can they be handled using the same crossover and mutation schemes. Therefore, they are separately processed in two sub-strings $X_1^{(z)}$ and $X_2^{(z)}$ of individual z. It is noted that for $X_1^{(z)}$, a base-$(N-1)$ operation [43] is used to generate the integers from 0 to $(N-2)$, and then added by 1 to satisfy the constraint (15b). GA is implemented by a sequence of main operators including reproduction/selection, crossover, and mutation, repeatedly until satisfying one of the two termination conditions (TC) given as follows:

- The average penalty value per individual derived from (19) is less than 10^{-3} in 10 consecutive generations.
- Generation count (Gen) is equal to a given number of generations ($N_{\text{G}} = 100$).

As an adaptive heuristic search algorithm, the time and memory complexity of Algorithm 2 is primarily determined by the population size N_{P} and the number of generations N_{G}. The values of N_{P} and N_{G} may vary depending on several factors, including: 1) the system scale characterized by M, N and I; 2) the computational burden associated with the objective function, constraints, and optimization variables in (15); and 3) the accuracy requirements of video streaming A&Ss.

Algorithm 2 GA for CAHO.

Require: System and GA parameters in Tables III and Table IV
$Gen = 1$: Generation count
Ensure: $T_F^*(h_i^*, c_{n,i}^*, b_n^*)$

1: Randomly generate
1) N_{P} sub-strings $\{X_1^{(z)}\}$, $z = 1, 2, ..., N_P$, each of I integer optimization variables $\{h_i\}$.
2) N_{P} sub-strings $\{X_2^{(z)}\}$, each of $(N \times I + N)$ bits to characterize a set of $N \times I$ binary optimization variables $\{c_{n,i}\}$ and N binary optimization variables $\{b_n\}$.
2: Compute N_{P} fitness values based on (20) to have $\{T_F^{(z)}\}$, i.e., $T_F^{(z)}\big(X_1^{(z)}, X_2^{(z)}\big)$.
3: **while** TC does not hold **do**
4: Put $\{X^{(z)}\} = [\{X_1^{(z)}\}\{X_2^{(z)}\}]$ associated with $T_F^{(z)}$ into the mating pool for ranking.
5: Select $N_{\text{PG}} = N_{\text{P}} \times P_{\text{G}}$ best individuals with lowest fitness values by using stochastic universal sampling operator [43] for breeding to obtain $\{X^{(t)}\} = [\{X_1^{(t)}\}\{X_2^{(t)}\}]$, $t = 1, 2, ..., N_{\text{PG}}$.
6: Choose a pair of parents to create the offsprings by using single point crossover with probabilities P_{ci} and P_{cb} applied to $\{X_1^{(t)}\}$ and $\{X_2^{(t)}\}$, respectively.
7: Mutate the offsprings $\{X_1^t\}$ and $\{X_2^t\}$ respectively with probabilities P_{mi} and P_{mb} by using complement operation so that the positive genetic features probably lost in the previous steps can be recovered to obtain $\{X^{(t),*}\} = [\{X_1^{(t),*}\}\{X_2^{(t),*}\}]$.
8: Repeat step 2 to obtain $T_F^{(t),*}\big(X_1^{(t),*}, X_2^{(t),*}\big)$.
9: Reinsert $\{X^{(t),*}\}$ and $T_F^{(t),*}$ into the present generation to obtain the new sets of $\{X^{(z)}\}$ and $T_F^{(z)}$.
10: $Gen = Gen + 1$
11: **end while**
12: Find the best fitness $T_F^*(h_i^*, c_{n,i}^*, b_n^*) \in \{T_F^{(z)}\big(X_1^{(z)}, X_2^{(z)}\big)\}$.

Table III
System and GA Parameters

Symbols	Specifications
M	5 UAVs
N	25 RSUs
K	7 zones covered by each RSU
I	10 videos
S_i	Uniformly random distributed from 0.25 to 2.5 (Gbit)
s_n	Uniformly random distributed from 30 to 60 (km/h)
d	250 m
λ	0.025 VUs/m
α	1
δ	0.5
W	10 MHz
P	5 W
σ^2	10^{-12} W
c	3×10^8 m/s
f_c	2 GHz
$\{\rho_1, \rho_2\}$	$\{10^{-6}, 1\}$, constraint violation degree properly determined based on the approach proposed in [40]
N_{P}	3000 individuals
N_{G}	100 generations
P_{G}	0.9, 90% of the individuals with the lowest fitness values are selected for breeding
$\{P_{\mathrm{ci}}, P_{\mathrm{cb}}\}$	{0.9, 0.6}, set to sufficiently high values to ensure effective crossover and convergence
$\{P_{\mathrm{mi}}, P_{\mathrm{mb}}\}$	$\{10^{-12}, 10^{-12}\}$, set to sufficiently low values to ensure effective mutation and convergence

Moreover, the overall complexity is also affected by the implementation of genetic operators such as selection, crossover, and mutation. Consequently, the complexity of Algorithm 2 is on the order of $\mathcal{O}(N_{\mathrm{P}} N_{\mathrm{G}})$ [36, 40].

In practice, Algorithm 2 is more suitably executed at a single MBS, which centrally implements the CAHO strategy for all RSUs, UAVs, and popular videos within a limited road. Nevertheless, when the system scales up with longer road consisting of larger values of M, N, and I, practical deployment of CAHO faces two major challenges. On the one hand, acquiring the system information, such as channel state information, for formulating the CAHO optimization problem becomes increasingly difficult. On the other hand, the complexity of Algorithm 2 grows substantially. To overcome these challenges, the number of RSUs, UAVs, and popular videos assigned to each MBS should be carefully selected in accordance with the system scale and the processing capability of the MBS. Moreover, for scenarios involving large-size videos, multiple MBSs can collaboratively provide continuous video streaming A&Ss to RVs [24].

5 Performance Evaluation

5.1 Parameters Setting

The system and GA parameters are detailed in Table III. The propagation features of communication environments in different segments, which are randomly selected, are shown in Table IV. To evaluate the performance of CAHO method, we compare it with the other four schemes, including (i) random hovering (RAHO), (ii) random caching at RSUs (RACR), (iii) random caching at UAVs (RACU), and (iv) none-UAV deployment (NUAV), with different considered optimization variables as listed in Table V. In RAHO, h_i and $c_{n,i}$ are optimized, but b_n is randomly generated. In RACR, $c_{n,i}$ and b_n are optimized, but h_i is randomly generated. In RACU, h_i and b_n are optimized, but $c_{n,i}$ is randomly generated. And in NUAV, no UAVs are deployed ($M = 0$). Obviously, the constraints in all RAHO, RACR, RACU, and NUAV have to be satisfied. Furthermore, we force the RAHO, RACR, RACU, and NUAV to cache as much storage as or (a little bit higher storage than) the CAHO method does to ensure a fair comparison.

Table IV
Propagation Features [11, 34]

Environments \ Parameters	κ_n	ν_n	η_n^{LoS}	η_n^{NLoS}	θ_n
Suburban	4.88	0.43	0.1	21	20.34°
Urban	9.61	0.16	1	20	42.44°
Dense urban	12.08	0.11	1.6	23	54.62°
High-rise urban	27.23	0.08	2.3	34	75.52°

Table V
OVs of Different Schemes

Schemes \ OVs	h_i	$c_{n,i}$	b_n
RAHO	✓	✓	✗
RACR	✗	✓	✓
RACU	✓	✗	✓
NUAV	✓	✗	✗
CAHO	✓	✓	✓

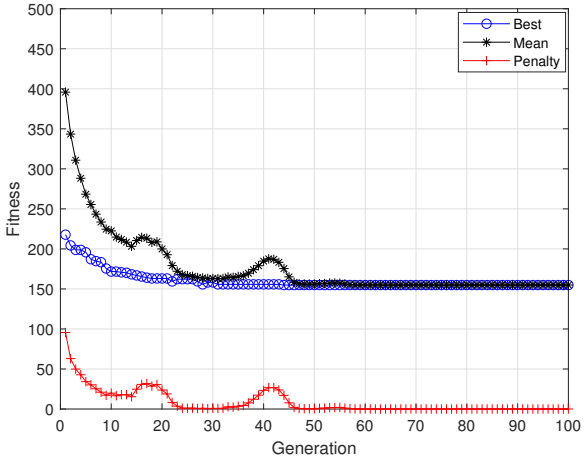

Figure 4. Convergence rate of GA.

5.2 GA Evaluation

Figure 4 illustrates the convergence behavior of GA in terms of the best fitness value (Best), the mean fitness value (Mean) defined in (20), and the average penalty

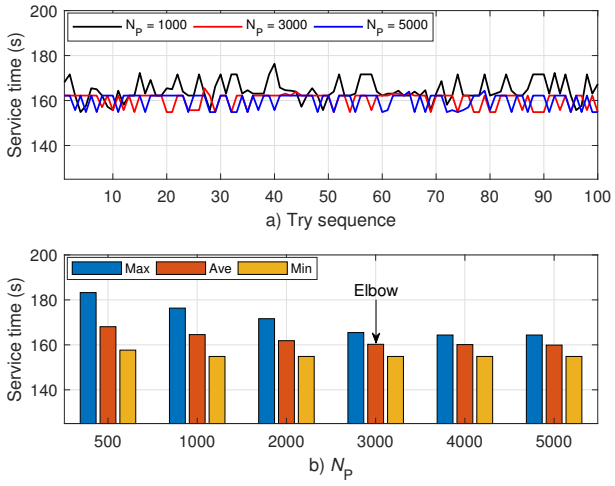

Figure 5. Convergence rate of GA.

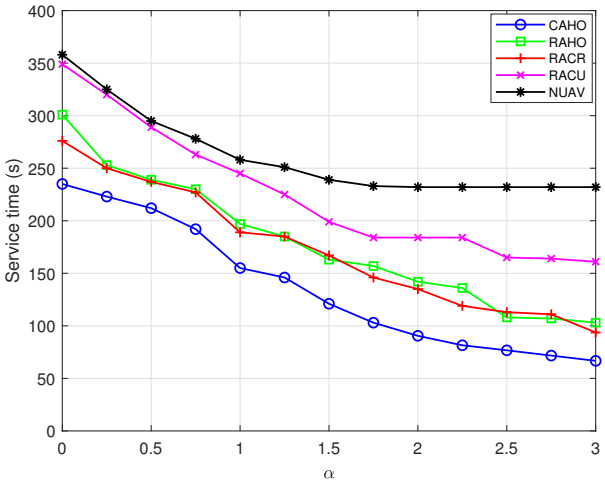

Figure 6. Service time performance versus α.

value (Penalty) defined in (19) across all individuals, versus the number of generations N_G. In the early generations, the large gap between the Best and Mean values indicates a high population diversity, reflecting that GA is strong capability to effectively explore the searching space. As N_G increases, both the Best and Mean values gradually decrease and approach each other, demonstrating the convergence process of GA. Although the Best and Mean values become sufficiently close from around the 30th generation, the GA continues to further minimize the fitness function while driving the penalty term to zero, thereby ensuring that all constraints of the CAHO optimization problem are satisfied. After about 45 generations, the Mean converges to the Best and remains stable until the final generation, indicating that the GA reaches an optimal or approximately optimal solution. In addition, the rapid decrease of the Penalty toward zero confirms the feasibility of the final solution with respect to the system constraints.

Besides the aforementioned convergence behavior for identifying the optimal solution, the stability and accuracy of GA are validated by executing the algorithm 100 independent tries for each population size ($N_P = \{500, 1000, 2000, 3000, 4000, 5000\}$), as illustrated in Figure 5. In Figure 5(a), for a small population size ($N_P = 1000$), the service time becomes more unstable and frequently takes higher values compared to the other two population sizes ($N_P = 3000, 5000$). As N_P increases to 3000 and 5000, the service time demonstrates significantly improved stability, with more accurate minimum values observed. To investigate the accuracy of GA, we further compute the maximum (Max), average (Ave), and minimum (Min) service time values over 100 independent tries for different population sizes as shown in Figure 5(b). For $N_P = 500$, the number of individuals is too small such that it cannot yield any accurate minimum values. A larger population size leads to a higher occurrence of accurate minimum values within 100 tries, thereby reducing the gap between the Ave and the Min. The results show

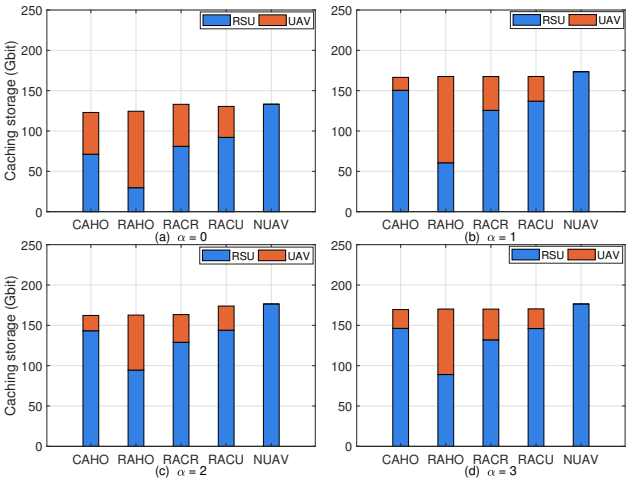

Figure 7. Caching storage performance versus α.

that this improvement is marginal when $N_P > 3000$. Increasing the population size beyond 3000 does not yield significant gains in service time, while incurring a rapidly increasing computational cost. The elbow point at $N_P = 3000$ indicates an appropriate population size, at which GA achieves high accuracy with a reasonable cost. These results confirm the feasibility and effectiveness of GA in practical scenarios, achieving a good balance between accuracy and computational cost.

5.3 CAHO Performance Evaluation

5.3.1 Performance versus α: Figure 6 plots the service time of different schemes versus α. As α increases, the service time of all schemes decreases, demonstrating the benefit of utilizing the caching resources for the most popular videos. CAHO achieves superior performance with the lowest service time by jointly optimizing all the three key OVs: caching radius at RSUs (h_i), caching placement at a UAV when it hovers over segment n ($c_{n,i}$), and hovering positions (b_n). Next to CAHO, RAHO and RACR provide comparable

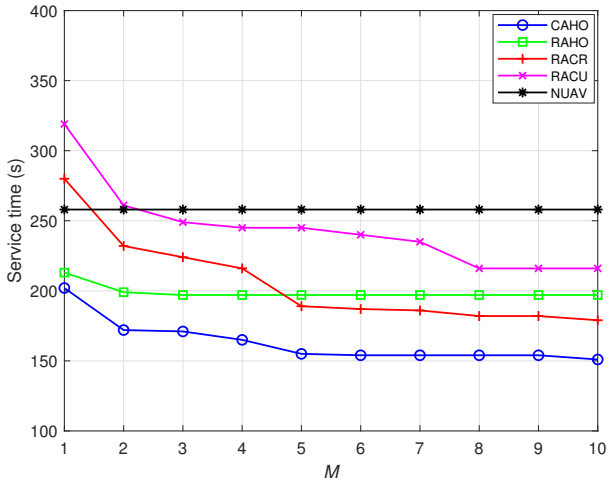

Figure 8. Service time performance versus M.

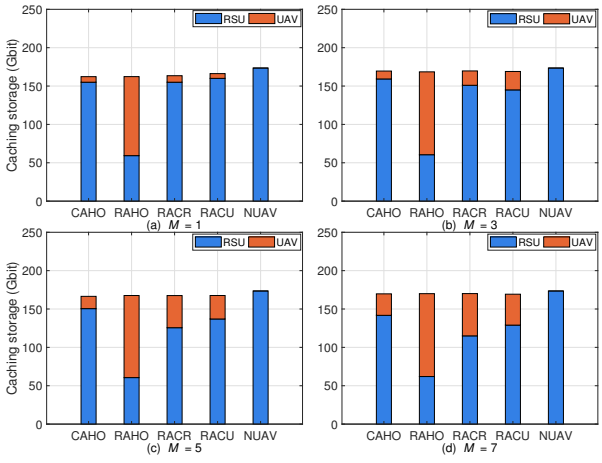

Figure 9. Caching storage performance versus M.

performance, suggesting that UAV hovering and RSU caching play equivalent roles in service time reduction. From the performance of RACU, it can be observed that UAV caching is more critical than UAV hovering or RSU caching, as random UAV caching incurs a longer service time compared to random UAV hovering (RAHO) and random RSU caching (RACR). Finally, the assistance of UAVs contributes the most to system performance, since the NUAV scheme, which excludes both UAV hovering and UAV caching, yields the worst service time among all schemes.

Concerning caching storage consumption, Figure 7 plots the relationship between storage consumed by CAHO, RAHO, RACR, RACU, and NUAV versus α. The five schemes achieve similar total storage consumption amounts, in which CAHO provides a slightly lower level, ensuring the fairness in comparison. The main difference lies in how the total storage resource is allocated between RSUs and UAVs among the schemes. As α increases, UAVs equipped with hovering and caching tend to concentrate their caching on a smaller set of highly popular videos, thereby shifting storage usage toward RSUs rather than UAVs, except for the NUAV scheme. Among the schemes, CAHO utilizes the storage resource most efficiently. In contrast, RAHO suffers the lowest efficiency because the UAV hovering positions are randomly selected, which forces the UAVs to cache more videos trying to reduce the service time and compensate for the inefficiency in hovering.

5.3.2 Performance versus M: Figure 8 shows the service time of CAHO, RAHO, RACR, RACU, and NUAV versus the number of UAVs M. It is evident that the service time decreases as the number of UAVs increases for all UAV-assisted schemes. When M becomes large, further increasing the number of UAVs leads to service time saturation due to the limited storage resource and caching gaps. RAHO reaches saturation more quickly because the UAV hovering positions are not optimized, which hinders the effective utilization of a large number of UAVs for service time reduction compared with RACR. Since NUAV does not employ UAVs, its performance remains unchanged with respect to M. Compared with other schemes, CAHO exploits additional UAVs more effectively, resulting in the lowest service

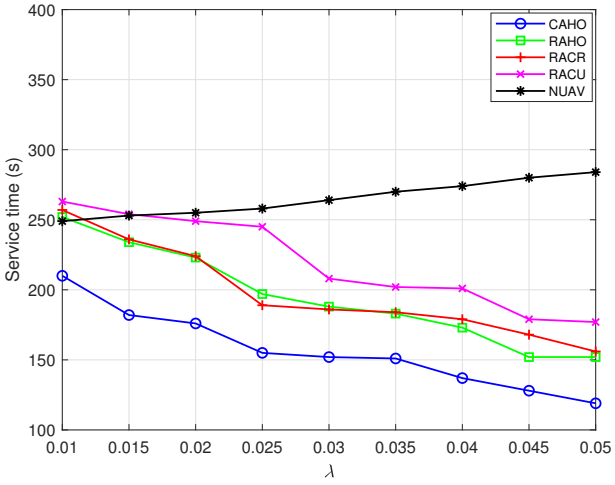

Figure 10. Service time performance versus λ.

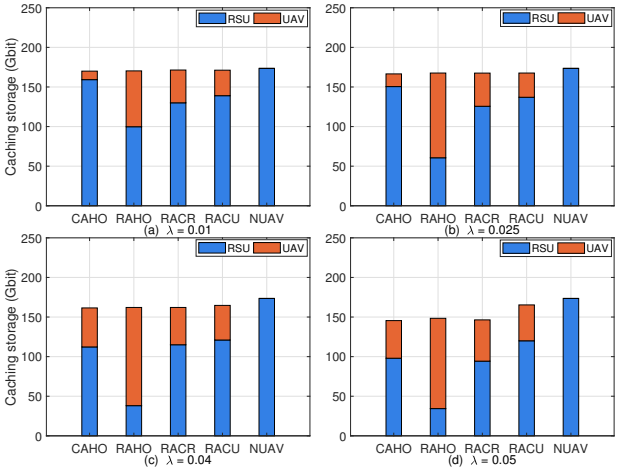

Figure 11. Caching storage performance versus λ.

time. Importantly, the number of UAVs should be chosen carefully for each VANET scenario, ideally at the saturation elbow point (e.g., $M = 5$). The caching storage consumption of all schemes with respect to M is investigated in Figure 9, in which the behavior is similar to that in Figure 7. In addition, it is clear that as M increases, UAVs utilize more opportunities to achieve better U2V transmission capacity for filling the caching gaps, leading to an increase in the caching storage consumed at UAVs.

5.3.3 Performance versus λ: The service time performance of all schemes versus the density of VUs λ is presented in Figure 10. The results show that for UAV-assisted schemes, the service time generally decreases with increasing λ. However, NUAV exhibits the opposite behavior because expression (5), divided by $V_{k,i}$, increases as λ grows. A higher density of VUs increases the probability of having RVs and enables leveraging the advantages of U2V channels in UAV-assisted schemes, thereby compensating for the limitations of R2V channels in NUAV. Consequently, UAVs consume more caching storage resources as λ increases, as shown in Figure 11. Overall, the comparisons and analyses of system performance for all schemes with respect to α, M, and λ indicate similar behaviors, where CAHO consistently provides the RVs with the lowest service time and efficiently utilizes the caching storage resources.

6 Conclusion

In this paper, we have proposed the caching and hovering (CAHO) optimization design for cooperative video streaming in UAV-assisted VANETs. By jointly determining the cache placement at RSUs and UAVs along with UAV hovering positions, CAHO addresses the caching gaps and adapts to varying content popularity pattern, number of UAVs, and vehicle distributions. Comparative evaluations against the other benchmark schemes including RAHO, RACR, RACU, and NUAV, demonstrate that CAHO consistently achieves the lowest service time and efficiently balances the storage allocation between the RSUs and UAVs. GA employed to solve the CAHO optimization problem enables effective exploration of the joint optimization space and provides stable convergence behavior with high accuracy under appropriate population sizes, facilitating performance evaluation of the proposed framework. The results further highlight that UAVs are effectively utilized to complement RSU caching without overuse and can adapt well to system variations in latency-sensitive video streaming A&Ss in dynamic VANET environments. As a promising direction for future work, learning-based, lower-complexity and adaptive optimization algorithms will be investigated with insightful comparison to further capture the fast time-scale dynamics in highly mobile vehicular environments and to enhance system adaptability under rapidly changing network conditions.

Acknowledgment

This research is funded by Vietnam National Foundation for Science and Technology Development (NAFOSTED) under grant number 102.04-2023.25.

References

[1] Cisco, "Cisco visual networking index: Global mobile data traffic forecast update," in *2017–2022 White Paper*, [Online]. Available: https://www.cisco.com, Feb. 2019.

[2] Cisco, "Cisco annual internet report," in *2018–2023 White Paper*, [Online]. Available: https://www.cisco.com, Mar. 2020.

[3] H. Feng, S. Guo, L. Yang, and Y. Yang, "Collaborative data caching and computation offloading for multi-service mobile edge computing," *IEEE Transactions on Vehicular Technology*, vol. 70, no. 9, pp. 9408–9422, Sep. 2021.

[4] Z. Ning, K. Zhang, X. Wang, L. Guo, X. Hu, J. Huang, B. Hu, and R. Y. K. Kwok, "Intelligent edge computing in Internet of vehicles: A joint computation offloading and caching solution," *IEEE Transactions on Intelligent Transportation Systems*, vol. 22, no. 4, pp. 2212–2225, Apr. 2021.

[5] J. Chen, H. Wu, P. Yang, F. Lyu, and X. Shen, "Cooperative edge caching with location-based and popular contents for vehicular networks," *IEEE Transactions on Vehicular Technology*, vol. 69, no. 9, pp. 10 291–10 305, Sep. 2020.

[6] S. Berri, J. Zhang, B. Bensaou, and H. Labiod, "Joint content-prefetching, transmission scheduling, and rate adaptation in vehicular networks," *IEEE Transactions on Vehicular Technology*, vol. 71, no. 4, pp. 4348–4358, Apr. 2022.

[7] Q.-A. Nguyen, N.-S. Vo, T. C. Lam, T. Do-Duy, H. Jung, and T. Q. Duong, "Joint deterministic and probabilistic edge caching minimized service time for cooperative video transmission in VANETs," *IEEE Transactions on Network Science and Engineering*, vol. 13, pp. 1932–1943, Sep. 2025.

[8] P. Wu, X. Yuan, Y. Hu, and A. Schmeink, "UAV-enabled covert autonomous vehicular communication: Joint trajectory and resource allocation design," *IEEE Transactions on Intelligent Transportation Systems*, vol. 6, no. 12, pp. 21 769–21 783, Dec. 2025.

[9] E. M. Mohamed, M. A. Alnakhli, and H. S. Hussein, "Contextual neural bandit approach for UAV selection in delay-doppler-based vehicular networks," *IEEE Wireless Communications Letters*, vol. 14, no. 11, pp. 3690–3694, Nov. 2025.

[10] M. Mozaffari, W. Saad, M. Bennis, Y. Nam, and M. Debbah, "A tutorial on UAVs for wireless networks: Applications, challenges, and open problems," *IEEE Communications Surveys and Tutorials*, vol. 21, no. 3, pp. 2334–2360, Third-quarter 2019.

[11] R. I. Bor-Yaliniz, A. El-Keyi, and H. Yanikomeroglu, "Efficient 3-D placement of an aerial base station in next generation cellular networks," in *Proceedings of the 2016 IEEE International Conference on Communications (ICC)*, Kuala Lumpur, Malaysia, May 2016, pp. 1–5.

[12] A. Hourani, S. Kandeepan, and A. Jamalipour, "Modeling air-to-ground path loss for low altitude platforms in urban environments," in *Proceedings of the 2014 IEEE Global Communications Conference*, Austin, TX, Dec. 2014, pp. 1–7.

[13] Z. Fan, M. Zhang, Y. Cao, Z. Liu, O. Kaiwartya, and Y. Javed, "A novel UAV-assisted VANET routing protocol for post-disaster emergency communications," *IEEE Transactions on Network Science and Engineering*, vol. 13, pp. 4863–4882, Dec. 2025.

[14] Y. Shin, H.-S. Choi, Y. Nam, and E. Lee, "Particle swarm optimization-based content delivery protocol for UAV VANETs," *IEEE Access*, vol. 13, pp. 1594–1608, Dec. 2024.
[15] X. Fan, H. Zhang, Y. Huang, Y. Su, H. Li, and J. Huo, "Temporal data dissemination in UAV-assisted VANETs through time-varying graphs," *IEEE Transactions on Vehicular Technology*, vol. 73, no. 10, pp. 14 835–14 846, Oct. 2024.
[16] K. Xiao, K. Feng, A. Dong, and Z. Mei, "Efficient data dissemination strategy for UAV in UAV-assisted VANETs," *IEEE Access*, vol. 11, pp. 40 809–40 819, Apr. 2023.
[17] A. Al-Hilo *et al.*, "UAV-assisted content delivery in intelligent transportation systems-joint trajectory planning and cache management," *IEEE Transactions on Intelligent Transportation Systems*, vol. 22, no. 8, pp. 5155–5167, Aug. 2021.
[18] G. Chen, Y. Han, F. Shen, Q. Zeng, and Y.-D. Zhang, "Edge collaborative caching based on incentive-driven D3QN combined with user preferences in UAV-assisted vehicular networks," *IEEE Transactions on Intelligent Transportation Systems*, vol. 26, no. 12, pp. 22 945–22 961, Dec. 2025.
[19] W. Wang, X. Xu, M. Bilal, M. Khan, and Y. Xing, "UAV-assisted content caching for human-centric consumer applications in IoV," *IEEE Transactions on Consumer Electronics*, vol. 70, no. 1, pp. 927–938, Feb. 2024.
[20] C. Li, K. Jiang, Z. Zhang, C. Xiong, and S. Wan, "Joint service caching and computation offloading scheme with 3D UAV deployment for ICVs in UAV-assisted VEC," *IEEE Transactions on Communications*, vol. 73, no. 11, pp. 10 886–10 899, Nov. 2025.
[21] Y. Liu, C. Yang, X. Chen, and F. Wu, "Joint hybrid caching and replacement scheme for UAV-assisted vehicular edge computing networks," *IEEE Transactions on Intelligent Vehicles*, vol. 9, no. 1, pp. 866–878, Jan. 2024.
[22] J. P. Jeyaraj, M. Haenggi, A. H. Sakr, and H. Lu, "The transdimensional poisson process for vehicular network analysis," *IEEE Transactions on Wireless Communications*, vol. 20, no. 12, pp. 8023–8038, Dec. 2021.
[23] S. Zhao, Y. Zhang, Y. Zhu, Z. Zhao, and Y. Liu, "Optimal probabilistic collaborative caching in UAV-assisted vehicular networks," in *Proceedings of the 2022 IEEE 25th International Conference on Intelligent Transportation Systems (ITSC)*, Macau, China, Oct. 2022, pp. 1–6.
[24] B. Feng, C. Feng, D. Feng, Y. Wu, and X.-G. Xia, "Proactive content caching scheme in urban vehicular networks," *IEEE Transactions on Communications*, vol. 71, no. 7, pp. 4165–4180, July 2023.
[25] L. Jiao *et al.*, "Performance analysis of uplink/downlink decoupled access in cellular-V2X networks," *IEEE Transactions on Mobile Computing*, vol. 23, no. 5, pp. 5616–5630, May 2024.
[26] K. Pandey, K. R. Perumalla, A. K. Gupta, and H. S. Dhillon, "Fundamentals of vehicular communication networks with vehicle platoons," *IEEE Transactions on Wireless Communications*, vol. 22, no. 12, pp. 8634–8649, Dec. 2023.
[27] V. V. Chetlur and H. S. Dhillon, "Success probability and area spectral efficiency of a VANET modeled as a Cox process," *IEEE Wireless Communications Letters*, vol. 7, no. 5, pp. 856–859, Oct. 2018.
[28] V. V. Chetlur and H. S. Dhillon, "Coverage analysis of a vehicular network modeled as Cox process driven by poisson line process," *IEEE Transactions on Wireless Communications*, vol. 17, no. 7, pp. 4401–4416, July 2018.
[29] L. Breslau, P. Cao, L. Fan, G. Phillips, and S. Shenker, "Web caching and zipf-like distributions: Evidence and implications," in *Proceedings of the IEEE INFOCOM'99. Conference on Computer Communications*, New York, NY, Mar. 1999, pp. 126–134.
[30] W. Xu, W. Shi, F. Lyu, H. Zhou, N. Cheng, and X. Shen, "Throughput analysis of vehicular Internet access via roadside WiFi hotspot," *IEEE Transactions on Vehicular Technology*, vol. 68, no. 4, p. 3980–3991, Apr. 2019.
[31] W. Saad, M. Bennis, M. Mozaffari, and X. Lin, *"Chapter 7 in Wireless Communications and Networking for Unmanned Aerial Vehicles"*, 1st ed. Cambridge University Press, 2020.
[32] ITU-R, "Rec. p.1410-2 propagation data and prediction methods for the design of terrestrial broadband millimetric radio access systems," *Series, Radiowave propagation*, 2003.
[33] M.-H. T. Nguyen *et al.*, "Spectrum-sharing UAV-assisted mission-critical communication: Learning-aided real-time optimisation," *IEEE Access*, vol. 9, pp. 11 622–11 632, Jan. 2021.
[34] M. Alzenad, A. El-Keyi, and H. Yanikomeroglu, "3-D placement of an unmanned aerial vehicle base station for maximum coverage of users with different QoS requirements," *IEEE Wireless Communications Letters*, vol. 7, no. 1, pp. 38–41, Feb. 2018.
[35] S. Katoch, S. S. Chauhan, and V. Kumar, "A review on genetic algorithm: Past, present, and future," *Multimedia Tools and Applications*, vol. 80, pp. 8091–8126, 2021.
[36] X. Qi, S. Khattak, A. Zaib, and I. Khan, "Energy efficient resource allocation for 5G heterogeneous networks using genetic algorithm," *IEEE Access*, vol. 9, pp. 160 510–160 520, Nov. 2021.
[37] H. Li *et al.*, "Energy-efficient task offloading of edge-aided maritime UAV systems," *IEEE Transactions on Vehicular Technology*, vol. 72, no. 1, pp. 1116–1126, Jan. 2023.
[38] M. I. Mushtaq *et al.*, "Framework for optimized resource allocation in multi-user, multi-service, multi-device aerial networks," *IEEE Access*, vol. 12, pp. 54 866–54 878, Apr. 2024.
[39] T. Fang and L. P. Chau, "GOP-based channel rate allocation using genetic algorithm for scalable video streaming over error-prone networks," *IEEE Transactions on Image Processing*, vol. 15, no. 6, pp. 1323–1330, Jun. 2006.
[40] N.-S. Vo, T. Q. Duong, H. D. Tuan, and A. Kortun, "Optimal video streaming in dense 5G networks with D2D communications," *IEEE Access*, vol. 6, pp. 209–223, Oct. 2017.
[41] H. Zhang, X. Cao, J. K. L. Ho, and T. W. S. Chow, "Object-level video advertising: An optimization framework," *IEEE Transactions on Industrial Informatics*, vol. 13, no. 2, pp. 520–531, Apr. 2017.
[42] G. Lai, F. F. Leymarie, and W. Latham, "On mixed-initiative content creation for video games," *IEEE Transactions on Games*, vol. 14, no. 4, pp. 543–557, Dec. 2022.
[43] A. Chipperfield, P. Fleming, H. Pohlheim, and C. Fonseca, *"Genetic Algorithm TOOLBOX For Using with Matlab"*. Ver 1.2 Users Guide, University of Sheffield, 1994.

Quynh-Anh Nguyen received the B.E. degree in Electronics and Telecommunications from Ho Chi Minh City University of Transport, Vietnam, in 2008, and the M.Sc. degree in Mobile Communications from Télécom ParisTech, France, in 2012. She is currently pursuing the Ph.D. degree in Computer Science with the School of Computer Science and Artificial Intelligence, Duy Tan University, Vietnam. She is with the Faculty of Electrical and Electronics Engineering, Vietnam Aviation Academy, Vietnam. Her research interests include wireless communications, vehicular ad hoc networks (VANETs), UAV-assisted communications, and next-generation mobile networks.

Nguyen-Son Vo received the B.E. and M.E. degrees in electronics and telecommunications from Ho Chi Minh City University of Technology, VNU-HCM, Ho Chi Minh City, Vietnam, in 2002 and 2005, respectively, and the Ph.D. degree in communication and information systems from the Huazhong University of Science and Technology, Wuhan, China, in 2012. He is currently with the Institute of Fundamental and Applied Sciences, Duy Tan University, Ho Chi Minh City. His research interests include content caching and delivering in wireless networks, multimedia wireless communications, quality of experience, and sustainability provision in wireless networks for smart cities, and for disaster and environment management. He was a recipient of the Best Paper Award at the IEEE Global Communications Conference 2016 and the prestigious Newton Prize 2017.

Van-Ca Phan received the B.E. and M.E. degrees in Electronics and Telecommunications from Ho Chi Minh City University of Technology, VNU-HCM, Vietnam, in 2002 and 2005, respectively, and the Ph.D. degree in Electronics and Radio Engineering from Kyung Hee University, South Korea, in 2011. He is currently an Associate Professor in the Faculty of Electrical and Electronics Engineering at Ho Chi Minh City University of Technology and Engineering, Vietnam. His research interests encompass wireless sensor networks, wireless and mobile communications, the Internet of Things (IoT), energy-efficient protocol design, and the integration of machine learning into wireless systems. Currently, his research focuses on cutting-edge projects in edge computing for video delivery systems in 6G networks and optimizing protocols for ultra-dense wireless environments, driving innovation in next-generation wireless communication technologies.

Dac-Binh Ha received the B.S. degree in Radio Technique, the M.Sc. and Ph.D. degree in Communication and Information System from Huazhong University of Science and Technology (HUST), China in 1997, 2006, and 2009, respectively. He is currently Associate Professor of School of Engineering and Technology at Duy Tan University, Da Nang, Vietnam. His research interests are secrecy physical layer communications, cooperative communications, cognitive radio, RF energy harvesting networks, B5G/6G networks, mobile edge computing, quantum computing and communications.

Minh-Phung Bui received the Bachelor of Informatics degree from Van Lang University, Vietnam, in 2000, the M.S. degree in Computer Science from the University of Information Technology, VNU-HCM, in 2010, and the Ph.D. degree in Computer Science from Duy Tan University, Vietnam, in 2022. He is currently the Vice Dean of the Faculty of Information Technology at Van Lang University, Ho Chi Minh City, Vietnam. His research interests include UAV-assisted IoT networks, energy-efficient routing in wireless sensor networks, multimedia wireless communication, and optimizing video storage and distribution systems.

Long D. Nguyen [S'16, M'24] received his Ph.D. degree in Electronics and Electrical Engineering from Queen's Univerisity Belfast (QUB), UK, in 2018. He was a Research Fellow at Queen's University Belfast, UK for a part of Newton project (2018-2019). He is currently with the Department of Engineering, Dong Nai University as an Assistant Professor and Duy Tan University as an Adjunct Assistant Professor in Vietnam. He is serving as a reviewer for some IEEE Transactions, international journals and conferences. Dr. Nguyen was awarded the Best Paper Award at the IEEE Digital Signal Processing (DSP) 2017, the IEEE International Conference on Recent Advances in Signal Processing, Telecommunication and Computing (SigTelCom) 2018, the IEEE International Conference on Communications (ICC) 2019, the International Wireless Communications & Mobile Computing Conference (IWCMC) 2019 and the IEEE Global Communications Conference (GLOBECOM) 2019, 2022. He was also awarded the Exemplary Reviewer Award in IEEE Communications Letters 2018 and 1st Prize "Technical Innovation" in the field of Information Technology - Electronics - Telecommunications, Dong Nai Province in 2023. His areas of interest in research of smart world include real-time convex/nonconvex optimization for real-world problem-solving (wireless communications, resource allocation, internet of things), digital transformation (data analysis, machine learning) modern computing (cloud computing, quantum computing) and embedded systems.